INTERNATIONAL ATOMIC ENERGY AGENCY
UNITED NATIONS EDUCATIONAL, SCIENTIFIC AND CULTURAL ORGANIZATION

INTERNATIONAL CENTRE FOR THEORETICAL PHYSICS
34100 TRIESTE (ITALY) - P.O.B. 586 - MIRAMARE - STRADA COSTIERA 11 - TELEPHONES: 224281/2/3/4/5/6
CABLE: CENTRATOM - TELEX 460392-I

SMR/115 - 36*

WINTER COLLEGE ON LASERS, ATOMIC AND MOLECULAR PHYSICS

(21 January - 22 March 1985)

Topical Meeting on the Free Electron Laser

THE STORAGE RING LASER

J.M. ORTEGA
L.U.R.E.
Université de Paris-Sud
Bat. 209-C
91405 Orsay Cedex
France

Topical Meeting on FELs → § 12-1, 12-3-a, 12-4, 12-5, 12-6, 12-7

DRAFT

January 1985

North-Holland FEL Handbook

Chapter 12

The Storage Ring Laser

D. A. G. Deacon

Deacon Research

754 Duncardine Way, Sunnyvale, CA 94087, USA

J. M. Ortega*

LURE

Batiment 209C, Universite de Paris Sud, 91405 Orsay, FRANCE

*Permanent Address: Ecole Superieure de Physique et Chimie
10 Rue Vauquelin, 75231 Paris Cedex, FRANCE

12.1 Introduction

The electron storage ring has several characteristics which uniquely qualify it as the driver of choice for many free electron laser applications. Principal among these is the extremely high normalized current density $\bar{i}/(\gamma e)^2$ (see chapter 2) available in state-of-the-art storage rings, which makes possible high gain operation, short wavelength operation, and possibly active guiding of the electromagnetic mode in the interaction region. The principal competitor drivers at this moment are the RF- and the induction- linear accelerators, which are limited by present technology to current densities four orders of magnitude lower than the storage ring. The linac driven laser system does promise higher power and efficiency since in the storage ring the laser power is limited to a fraction of the emitted synchrotron power. However, at the present time, the electron storage ring is the only source capable of serving the need for a high gain system for operation of the FEL at wavelengths in the visible region and below.

A great deal of information is now available on the operating characteristics of storage ring lasers thanks to the success of the LURE-Stanford collaboration at Orsay [1], and the contributions of the Novosibirsk [2], the Frascati [3], and the Brookhaven [4] groups. These experiments have shown that in many ways the storage ring system is easier to use than the linear accelerator based FELs: the high duty cycle of the beam makes possible the use of synchronous detection techniques for the measurement of small quantities impossible to extract from the noise on a pulsed system. Characterization of the electron beam is correspondingly improved, making possible detailed comparisons with the theory.

The short wavelength and the high duty cycle of the storage ring laser also suit it well to the spectroscopic, chemical, and other scientific applications [5] which will be the first beneficiaries of the FEL developments in this wavelength range. Furthermore, since the laser does not excite the emittance of the ring in its standard configuration, it seems likely that synchrotron radiation users will wish to use the beam at the same time as an operational free electron laser, provided that they do not require the smallest possible bunch lengths or energy spreads. This will permit multiple use of the stored beam when the laser operating schedule can be determined.

The storage ring systems also share some difficulties, the most bothersome of which is associated with the operation at short wavelength. The harmonics generated in all linear undulators (chapter 4) appear at short enough wavelengths so that they can create absorption centers in the dielectric materials making up multilayer laser mirrors. The protection of the oscillator mirrors is now the most serious problem facing the

operation of FELs in the visible and the UV regions [6]. The other ticklish problems associated with the operation of storage rings stem from the fact that the lifetime of the stored beam must be maintained at an acceptable level. This means an ultra high vacuum environment must be maintained in the ring, and a certain minimum aperture must be provided at the undulator. Although we can work around the latter constraints, some improvement is called for in our materials technology for application in the harmonic-rich UV FEL environment.

With existing storage ring technology it is possible to produce a normalized current density of $\hat{i}/(\gamma\epsilon)^2 = 10^8$ amp/cm^2-rad^2 with a low energy spread. (The emittance in a storage ring is defined as the product of the RMS beam size and angular content at a beam focus.) In an undulator of optimized length, such an electron beam can produce gain on the order of 10 per pass in any segment of the range 5000 A to 100 A. The main unknown factor which enters into the calculation of laser performance over this wavelength range is the quality of the mirrors which will be available [7]. Various schemes for making optimum use of the electron beam are now under active discussion, but it is clear that in some configuration, a storage ring laser is a viable device for the production of very short wavelength radiation. We expect that within the next three years such devices will be produced at Orsay in the intermediate gain regime, and at Stanford in the high gain regime.

The existence of high gain, in addition to making possible short wavelength operation, has other important implications. Once the radiation produced by the electron beam exceeds in amplitude the input field, the physics of the interaction can change markedly. The diffraction characteristics of the amplified wave become dominated by the electron beam and can become actively guided [8] by the amplifying medium. In such a situation, the free space modes become an inappropriate basis set by which to analyze the interaction, and the optimization of the system changes drastically. Secondly, the net gain in the high gain case increases due to exponential amplification. And finally, the inhomogeneous broadening terms (chapter 5) become smaller since the bunching required to amplify the light takes place a limited distance previous to an electron's instantaneous position. All of these effects increase the net gain in the laser and change the scaling relations for the optimization.

In this chapter, we describe the optimization of the small signal gain in a storage ring laser as prelude to the discussion of the ultimate wavelength limit of these machines with present technology. The present state of our experimental knowledge of these machines is explored through a review of the principal results of the existing experiments, and we conclude with an assessment of the major technological problems which remain to be solved, and a discussion of the outlook for the forseeable future

(5 years).

12.2 Optimization of the small signal gain

In the XUV and beyond, the best available mirrors [7] have reflection coefficients approaching 50% at normal incidence. In order to achieve laser operation, a net gain on the order of 400% is required to reach threshold since amplification occurs only once per round trip in the FEL. In this wavelength region, the primary device consideration must be to optimize the small signal gain so that the threshold condition can be reached. None of the free electron lasers to operate to date have achieved a gain higher than 100% due to a combination of factors including low electron beam quality and limited interaction length. If optimum use is made of the high normalized current density beam provided in the electron storage ring, it is possible not only to push out to the short wavelength region, which in itself reduces the gain (chapter 5), but also to increase the gain above the levels ever achieved before at much longer wavelength. We will examine the case in which the storage ring design is optimized for FEL operation.

The small signal gain (chapter 5) in a linear undulator is given by

$$G = \rho r_0 \lambda_0^2 F_{inh} F_f \frac{16\pi^2 \bar{K}^2 N^3 [JJ]^2}{\gamma^3} \qquad (12\text{-}1)$$

where

$$F_{inh} \equiv \left\langle \frac{1 - \cos\nu - \frac{\nu}{2}\sin\nu}{\nu^3} \right\rangle_{\text{phase space}}$$

This relation assumes a low divergence optical mode and electron beam. If the gain is low, the input power P is increased by the gain G to (1+G)P. If the gain is large, the amplification becomes exponential with a growth constant proportional to the third root of G. If the input wave is guided by the amplifying electron beam, or if the gain is large enough to reduce the inhomogeneous broadening, the net amplification will be further increased. Whether in the large or the small gain regime, an optimization of the small signal gain G results in the maximum system gain. This optimization must be carried out into a low divergence Gaussian mode for a low gain oscillator or amplifier, and into the self-consistent optical beam in the high gain guided wave case. The inclusion of the filling factor F_f [9] to take account of the overlap of the two beams is a good approximation in either case. In general, the propagation of the electron beam and of the charge density wave in that beam must be separately taken into account since the electron beam focussing can influence the dynamics of the interaction through changes in the phase of the electrons. However, in the optimum case considered below, the charge density wave is unaffected by the focussing of the electron beam, and the entire effects of the beam overlap

including scalloping can be taken into account in the filling factor.

Since the gain varies as the cube of the number of periods, the gain optimization demands the longest undulator subject to the constraints imposed by the finite emittance and energy spread of the beam, and by the propagation of the optical mode. We will discuss the length scaling after these effects have been discussed individually.

For a fixed length system operated at a given energy and wavelength, the gain varies as

$$G \propto \frac{\bar{K}^2}{\lambda_0} [JJ]^2 \qquad (12\text{-}2)$$

We wish therefore to reduce the wavelength λ_0 as much as possible and increase K to the maximum. Keeping the wavelength constant as we reduce λ_0 implies increasing K according to the resonance condition (chapter 5). However, it becomes technologically more and more difficult to produce high magnetic fields at short λ_0 and we arrive at an optimum value of K and λ_0 set by our technological resources. The highest magnetic fields can be obtained by reducing the magnetic gap to the minimum acceptable value. In a storage ring system, the minimum gap is set by the need to maintain a long lifetime for the stored electrons. The pure rare-earth-cobalt undulator design suggested by Halbach (chapter 15) is a good one, and has been used by four out of the five FEL oscillators which have operated to date. The hybrid design offers a small improvement in field strength at the cost of the use of permeable materials with their attendant nonlinear response to external fields.

For the low gain case, the Rayleigh range must be set to a fraction of the undulator length [10], which we choose to be

$$z_0 = \frac{L}{\pi} \qquad (12\text{-}3)$$

If z_0 is too small, the divergence of the mode turns off the interaction before the end of the undulator, and if z_0 is too large, the mode waist becomes too large to couple well to the electron beam.

We now have the need to choose the electron beam envelope functions (the beta functions of chapter 14) in the undulator. The linear undulator produces a K-dependant focussing in the magnetic plane, and external focussing may also be imposed in and around the undulator. These functions and the emittance determine the electron beam size and angular spread, which must be optimized for minimum inhomogeneous broadening and maximum filling factor.

We assume in the following that cylindrical symmetry is

established in the interaction region. This implies that a uniform external focussing is applied in the wiggle plane and adjusted to produce equal focussing in the two transverse planes. This can be done, for instance, by alternately canting the pole faces to produce strong alternating gradient focussing. The focussing constant k_β, $(x'' + k_\beta^2 x = 0)$ is then

$$k_\beta = \frac{\bar{K} q}{\sqrt{2}\,\gamma} \qquad (12\text{-}4)$$

An arbitrary electron injected into this structure will execute oscillations in the two transverse planes such that the londitudinal velocity averaged over an undulator period remains constant. Furthermore, if the beam is injected focussed to a waist with a beta function of

$$\beta_{opt} = 1/k_\beta \qquad (12\text{-}5)$$

the electron beam envelope also remains constant. Other values of the input beta function will result in a scalloped electron beam

$$\beta(z) = \beta_{mid}\left[1 + \left(\frac{\beta_{opt}^2}{\beta_{mid}^2} - 1\right)\sin^2\frac{z}{\beta_{opt}}\right] \qquad (12\text{-}6)$$

where β_{mid} is the beta function at the symmetry point in the middle of the undulator.

For strong magnetic fields, β_{opt} becomes small and k_β becomes large so that one is obliged to set $\beta \simeq \beta_{opt}$. However, for weak undulator field strength, since k_β becomes small, one is no longer forced to match the beta functions. When β_{opt} grows larger than z_0, we can hold $\beta_{mid} = z_0$ (see equation (12-9)) and remain assured that the phase advance in (12-6) will be less than π and that the growth in the beam size from the center to the ends of the undulator will be less than 1.9, the value for a freely propagating beam. In what follows, we will therefore discuss two cases: one in which $\beta_{opt} > z_0$ so that we can set $\beta_{mid} = z_0$, and the other in which we set $\beta_{mid} = \beta_{opt}$.

For an electron beam with a given current, varying the dimensions changes both the on-axis electron density and the filling factor [9]. To maximize the product of the density and the filling factor, we require that the electron beam dimensions be equal to or smaller than the waist of the optical mode.

$$\sigma \le \frac{w_0}{2} \qquad (12\text{-}7)$$

To be sure that the inhomogeneous broadening is not too large, we require that the shift in the resonance parameter

$$\begin{aligned} \delta\nu &\equiv \delta\left\{L\left[(k+k_0)\beta_\parallel - k\right]\right\} \\ &\simeq -L(k+k_0)\frac{1}{2\gamma^2}\left(\delta\bar{K}^2 + \gamma^2\theta^2\right) \\ &= -L(k+k_0)\frac{1}{2\gamma^2}\left[\frac{\bar{K}^2 k_\beta^2}{2}(x^2+y^2) + \gamma^2(\theta_x^2+\theta_y^2)\right] \end{aligned} \qquad (12\text{-}8)$$

produced by the one standard deviation particle in the two transverse dimensions be less than π, which implies

$$\sigma_\theta^2 \le \frac{\lambda}{4L} \qquad (12\text{-}9)$$

These relations, with (12-2), are consistent with the requirement that the divergence of the electron beam in free space be less than or equal to that of a diffraction limited Gaussian optical beam.

$$\beta \gtrsim z_0 \qquad (12\text{-}10)$$

According to the above discussion, this restriction is appropriate when the focussing produced in the undulator is small enough

$$\sqrt{2}\,\bar{K} \le \frac{\gamma}{N} \qquad (12\text{-}11)$$

Physically, these equations describe an electron beam which is completely contained within a diffraction limited Gaussian mode. We note that this implies a certain minimum emittance for the beam. Equations (12-7) and (12-9) cannot be satisfied simultaneously unless

$$\varepsilon < \frac{\lambda}{4\pi} \qquad (12\text{-}12)$$

We see that the emittance of the electron beam limits the performance of an FEL in a very fundamental way. As the wavelength is reduced below the value $4\pi\varepsilon$, the gain begins to plunge (see for example figure 1, in which $\lambda = 4\pi\varepsilon$ at 1000 A). With the presently available values of peak current and mirror reflection coefficient, it becomes impossible to operate the laser much further than a factor of 5 or 10 in wavelength beyond the point where (12-12) is violated. The minimum wavelength for the operation of an FEL in the low gain region is therefore set primarily by the emittance of the beam, and secondarily by the peak current. This limitation can only be circumvented by establishing very high gain as discussed below so that the inhomogeneous effect caused by the emittance is reduced.

Let us assume that the laser wavelength is adjusted by changing the magnetic field of the undulator, keeping the electron energy constant. The wavelength is adjusted in the range between the lower limit set by (12-12), and the upper limit set by the maximum magnetic field technologically available. The optimization criteria change depending on whether (12-11) is true or false. In the short wavelength region we follow (12-10), and (12-9) inserted in the gain expression results in

$$G_{short} \approx \frac{\hat{I} r_0}{ce} F_{inh} \frac{32\pi^3 N^2}{\gamma} \frac{\bar{K}^2 [JJ]^2}{1+\bar{K}^2} \qquad (12\text{-}13)$$

where

$$\bar{K} \le \frac{\gamma}{N\sqrt{2}} \qquad \varepsilon = \frac{\lambda}{4\pi} \qquad \sigma = \frac{w_0}{2}$$

In the long wavelength region where (12-11) is false, we follow (12-5), and (12-9) results in

$$G_{long} = G_{short} \frac{2\left(\frac{\sqrt{2}\bar{K}N}{\gamma}\right)^2}{1+\left(\frac{\sqrt{2}\bar{K}N}{\gamma}\right)^2} \qquad (12\text{-}14)$$

where

$$\bar{K} > \frac{\gamma}{N\sqrt{2}} \qquad \varepsilon = \frac{\lambda}{4\pi}\frac{\gamma}{\sqrt{2}\bar{K}N} \qquad \sigma = \frac{w_0}{2}\frac{\gamma}{\sqrt{2}\bar{K}N}$$

It is clear that the gain now scales only quadratically in the length. At fixed energy, wavelength tuning is obtained through the magnetic field dependence; at large K, we observe that the gain is essentially independent of the wavelength.

The remaining factor in the inhomogeneous broadening is the energy spread, which does affect the choice of the maximum undulator length. The effect of the energy spread is to establish a minimum (inhomogenoeus) bandwidth for the emission process. Increasing the undulator length reduces the natural (homogeneous) bandwidth, thereby increasing the gain. Near the length at which these two bandwidths are equal,

$$L_{opt} = \frac{\lambda_0}{4\left(\frac{\sigma_\varepsilon}{E}\right)} \qquad (12\text{-}15)$$

the phase space average of (12-13) begins to reduce in size, and the gain ceases to grow quadratically in the length. At $L \simeq .7 \times L_{opt}$ the gain grows only linearly with the length, and by $L \simeq 3 \times L_{opt}$ no further improvement in the gain can be obtained. To find the optimum gain that can be obtained in this regime of operation, we set $L = L_{opt}$ and find

$$G_{short}^{opt} \approx \frac{\hat{I} r_0}{ce} \frac{\bar{K}^2 [JJ]^2}{\gamma\left(\frac{\sigma_\varepsilon}{E}\right)^2 (1+\bar{K}^2)} \qquad (12\text{-}16)$$

which varies inversely as the square of the energy spread.

The undulator described by (12-15) can be many meters in length. In order to observe the full quadratic enhancement of the gain as a function of length, the magnetic field configuration of the undulator must not have large or cumulative errors. Since for high quality electron beams the optimum undulator can be quite long, the constraints on the undulator fields become quite restrictive. The acceptable magnitude of the field errors varies inversely as the length. An important technological challenge for the field is to device methods for reducing the imperfections in undulator devices.

These imperfections reduce the gain and increase the spontaneous emission bandwidth. Fortunately, it is not necessary to measure the gain, which is difficult, in order to project the performance of a given device in the FEL oscillator. Using the Madey theorem [11] it is sufficient to measure the forward spontaneous emission spectrum, which is relatively simple. The Madey theorem and its limits have now been verified in detail as shown in figure 2.

Let us include the energy scaling of the electron beam parameters of the storage ring. The emittance scales as γ^2, the energy spread scales as γ, and the peak current, which is limited

by the Touschek lifetime, scales as γ^5. (The constants of proportionality depend on the lattice design and the operating point for the emittance, the size of the ring for the energy spread, and mainly on the RF voltage for the peak current.) The optimized gain therefore grows quadratically with the energy of the ring.

In order to obtain maximum gain in a storage ring FEL, a designer is therefore led to consider systems of the largest energy that he can afford subject to the requirement that resonance can be established in the wavelength range of interest. In order to maintain resonance, high values of magnetic field and long undulator wavelengths are required. However, since the energy spread increases linearly with the energy, the optimum undulator length actually decreases with energy once K becomes large.

The proposed Stanford-Deacon Research FEL program can serve as an example for the above considerations. The electron beam and the laser parameters are listed in Table I. The emittance of the

<u>HIBESS electron beam characteristics (design values)</u>

energy	1 GeV	
peak current	270 amp	(1 hr Touschek lifetime)

emittance	9×10^{-9} m-rad	(round beam)
energy spread	6×10^{-4}	
injection:	with e^+ or e^- at 1 GeV	

High gain, diffraction and guiding FEL experiment (HIDAG)

(preliminary values)

undulator length	28 m	(pure REC)
magnetic period	11 cm	(interchangeable)
maximum K	7.6	(gap = 30 mm)
laser wavelength	5000 → 1000 Å	(fundamental)

TABLE I

storage ring limits the wavelength of high gain operation to $\lambda \le$ 1000 Å from equation (12-12), and indeed we see in figure 1 that the gain begins to drop precipitously at this wavelength. The available straight section length is 60% of L_{opt}, which is reasonable given the high cost per unit length of building the undulator, and the declining benefits of increasing the length as L_{opt} is approached. From equation (12-13), the gain is $G \simeq 4.2$. As mentioned above, the exponential growth and possible some active guiding will produce a net amplification substantially larger than G.

Since the gain in a high energy storage ring is limited by the peak current, which is limited by the Touschek lifetime at high energy, it is possible to increase the gain by operating in a pulsed mode. The peak current can be increased as the square root of the RF voltage applied to the stored beam, until an instability threshold prevents further increase. (This is another reason to operate at high energy: all of the instability thresholds are higher.) To take the example of the HIBESS ring, if the current is increased to the kiloampere region where the longitudinal wake field instability is predicted to set in, bunch lengthening will occur, effectively preventing further increases in the peak current. The Touschek lifetime is very short (a few minutes) at this current. However, if the RF voltage is pulsed up for a time short compared to the Touschek lifetime, only small net beam loss will occur. This would allow repetitive pulsing into the very high gain regime as long as the duty cycle is low.

12.3 Alternatives to the Regular Undulator

12.3.a. The Optical Klystron

A modification of the undulator called the optical klystron [12] is often a useful device, particularly in storage rings due to their low energy spreads and often limited available straight section lengths. This device is composed of two undulators separated by a magnetic dispersive section, which acts to increase the available gain in a given length at the expense of the gain bandwidth. As such, it can only be of value if the length of the available interaction region is smaller than the optimum length (12-15). Use of the optical klystron under these conditions can increase the gain by as much as L_{opt}/L. By contrast, if the flexibility exists in the design stage of the storage ring laser system, the gain can be increased by the square of this ratio if an undulator of optimum length is installed on the same quality beam. If $L < L_{opt}/2$, and the energy spread is small enough, the optical klystron can be used to advantage; if the straight section can be designed at the optimum length, better performance will be obtained from an undulator.

Let us discuss the optimization of the optical klystron. Since most storage rings have not been optimized for F.E.L. studies, their straight section lengths are insufficient and the OK may be useful to enhance the gain. Following Elleaume's /18/ analysis, the OK can be characterized by the parameter N_d :

$$N_d = \frac{\gamma}{2\lambda}\frac{ds}{d\gamma} = \frac{L_d}{2\gamma^2\lambda} \quad (12.17)$$

when the dispersive section is simply a drift straight section

$$= \frac{1}{2\gamma^2\lambda}\left[L_d + \frac{e^2}{m^2c^2}\int\left(\int_{-\infty}^{u} B(z)\,dz\right)^2 du\right]$$

otherwise

The gain of the OK is :

$$G_{OK} = G_{und}\ (2N \text{ periods}) \times 0.93 \times \left(1 + \frac{Nd}{N}\right) f \qquad (12.18)$$

where

$$f = \exp - \left[2\sqrt{2}\,\pi\,(N + N_d)\,\frac{\sigma_\gamma}{\gamma}\,\frac{\lambda}{\lambda_R}\right]^2 \qquad (12.19)$$

where λ_R is the resonant wavelength and σ_γ/γ the energy spread of the ring. Physically f is the depth of the OK emission line modulation (due to the interference effect between the two N periods undulators).

12.19 is valid only as long as the longitudinal distribution of the electrons inside the bunch is gaussian. The maximum gain of the OK for the proper choice of N_d $\left(N_d = \left(4\pi\frac{\sigma_\gamma}{\gamma}\right)^{-1} - N\right)$ is:

$$G_{OK}^{max} = \frac{.045}{N\sigma_\gamma/\gamma}\ G_{max}\ (2N) \qquad (12.20)$$

It can also be shown that no extra gain is obtained by working on harmonics with an OK. The storage ring emittance broadens the envelope of the gain curve and consequently does not limit the OK as strongly as the energy spread (which broadens the fringes). Therefore the gain of the OK can be written :

$$G_{OK} \sim \left(\frac{L}{\gamma}\right)^3 \frac{K^2}{\lambda_0}\,\rho_e\,\frac{1}{N(\sigma_\gamma/\gamma)}\,[JJ]^2\,F_F \qquad (12.21)$$

In order to extract scaling information from this expression, let us make the following simplifications :

(i) For K not too small $\lambda \sim \frac{\lambda_o K^2}{\gamma^2}$

Then 12.21 becomes :

$$G_{OK} \sim [JJ] F_f \frac{L^2 \lambda \rho_e}{\gamma \lambda_o (\sigma_\gamma/\gamma)} \qquad (12.22)$$

(ii) For a given emitted wavelength, λ, a smaller λ_o is needed at lower energies. From our experience λ_o scales approximately as $\sim \gamma$

(iii) The energy spread $\frac{\sigma_\gamma}{\gamma}$ scales as γ on a given storage ring

(iv) The maximum achievable electronic density scales as $\rho_e \sim \gamma^\alpha$. If we consider only the Tousheck limitation on ρ_e, $\alpha \simeq 2 - 3$. However, for the OK the anomalous bunch lengthening threshold (above which the bunch and energy spread grow dramatically) is a more crucial parameter. The threshold scales approximately as $\sim \gamma$ with the stored current /19/. This lower α to $\sim 1 - 2$ (It would be unity if the bunch volume was kept constant at a given current while rising the energy) On the whole :

$$G_{OK} \sim L^2 \lambda \gamma^{-(3-\alpha)} F_f \; [JJ]^2 \qquad (12.23)$$

$[JJ]^2$ will be slightly improving while decreasing γ as K will decrease anf F_f will depend on the transverse bunch size used at different energies. However it can be concluded that the optical klystron gain optimization favors the lowest possible working energy as long as the Tousheck lifetime does not become too short and as the various instabilities which appear at low energy remain under control. Therefore finding the best operating parameter for the FEL of a given ring constitutes an important part of the work of a FEL designer.

As an illustration of this discussion we present in table II the estimated performance of a $\lambda_o \sim 10$ cm undulator placed on the storage ring super ACO, currently under construction (First electrons are planed for mid-1986). Although the design energy is 800 MeV the ring has been designed

in order to work also at low energies. The undulator period is rather long in order to be able to work in a large range of emitted wavelength and storage ring energies. The gain is given for a calculated point of operation at 400 MeV /15/.

TABLE II SUPER ACO ELECTRON BEAM CHARACTERISTICS AT 400 MeV (calculated).

Peak current	50 amp (90 mn Tousheck lifetime)
Emittance	$\varepsilon_x = 2.8 \; 10^{-8}$
Energy spread	$2.6 \; 10^{-4}$
R.F. freq.	500 MHz (120 harm. of the fundamental)
Injection	with e^+ or e^-
Bunch length	2.7 mm

POSSIBLE OPTICAL KLYSTRON FOR SUPER-ACO

Overall length	3.3 m
Magnetic period λ_o	$\sim$ 10 cm
Number of periods N (each undulator)	15
Nd (adjustable)	0 - 300
Maximum K	6
Expected wavelength range (400-800 MeV)	120 - 700 nm
Gain at λ = 150 nm (400 MeV - K = 1.3)	20 %

The lower limit of the expected wavelength range is determined mainly by the mirror reflectivity (see chapter 16) which drops rapidly below 120 nm (limit of the aluminium reflectivity). Let us point out that working at low energy and thus at low K has the further advantage of minimizing the mirror degradation which is due to the intense production of harmonics and XUV light by the undulator and dispersive section (see ref. 16, and below).

12.3.b. Transverse Gradient Undulator

The "transverse gradient wiggler" [13] is the opposite limit to the optical klystron in that it increases the gain bandwidth while reducing the amplitude of the gain. The value of this approach lies in the saturated regime of laser operation, a regime we consider below. By increasing the energy acceptance of the wiggler, more power can be extracted from the beam and the laser will operate more efficiently. It is clear, however, that there must already be plenty of gain available to turn the laser on and drive it to saturation before one could imagine trading in some of that gain for higher power and efficiency.

12.3.c. Isochronous Storage Ring Laser

A more radical modification of the physics of the FEL interaction has been proposed [14] in the isochronous storage ring laser. Here, the idea is to modify the optics of the storage ring so that the optical phase of the electron from pass to pass is maintained within a wavelength. This results in a steady state trapping of the electrons within the optical buckets much as described in Chapter 6 for the tapered wiggler and a single pass beam. The consequences which are projected for this mode of operation are strong, first order energy transfer into the laser since the electrons are prebunched, and high efficiency operation since no radiation damping is required to maintain the laser power. The technical difficulties [15] which must be resolved to build such a system are largely unknown to experimental practice since storage ring physicists have had no reason to attempt to build quasi-isochronous electron rings. However, as the new

storage rings at Orsay, Tsukuba, and Stanford become available for such work, we expect to see considerable effort applied to the realization of stable, quasi-isochronous optics.

12.3.d. High Gain Regime

Although we have based the present discussion on a consideration of the small signal gain using the small gain formula (12-1), some discussion is in order of the high gain regime, which presents some unique differences from the low gain physics. Once G becomes significantly larger than unity, three factors combine to increase the net amplification which would actually be observed. First, the wave begins to grow exponentially. Second, the effect of the emittance and energy spread of the electron beam is reduced since the length over which the bunching must be maintained is limited to approximately one e-folding distance. And third, the imaginary part of the gain tends to refocus the optical wave onto the electron beam, producing active guiding [8].

None of these phenomena have ever been seen because of the low gain available in the existing experiments. In the case of active guiding, the optimization of the interaction region takes on a radically different character from that presented above, the most notable being that there appears to be no limit on the length of an optimized undulator! As another very intriguing possibility, the combination of these three factors may permit the operation of a FEL in the X-Ray region in a kind of amplified spontaneous emission configuration [16]. In this proposal, no mirrors would be required; the spontaneous emission at the beginning of the undulator would be guided and amplified by a factor of a million or so in an exceedingly high gain undulator. This is proposed to be done in the X-Ray region by narrowing the undulator gap to a very small value, and increasing the number of periods. A small emittance beam is required for such a long, small gap undulator, so that a storage ring is used, and the lifetime is maintained by kicking the stored beam through the small gap undulator only a few times per second. Short of an improvement in our technology to permit the production of lower emittance electron beams, this approach offers the only hope of FEL operation at wavelengths shorter than 100 A or so.

We conclude that with available technology, operation from 5000 A through 1000 A can be achieved. The extent to which the oscillator configuration can be pushed below 1000 A will depend on how effective is the exponential gain in reducing the inhomogeneous broadening. It appears reasonable to project that FEL oscillators might eventually reach 100 A. The mirrorless amplified spontaneous configuration is probably capable of operation at significant power levels down to 25 A or so. Further progress would require significant improvement in the emittance.

TABLE III - ACO SRFEL CHARACTERISTICS

Storage ring ACO

Nominal energy	536 MeV
Laser working energy range	160 - 224 MeV
Circumference	22 m
Number of bunches	2
Electron beam current for oscillation	16 to 100 mAmp
RMS bunch transverse dimensions (σ_x & σ_y)	0.3 to 0.5 mm
RMS bunch length (σ_z)	0.5 to 1 nsec
RMS bunch relative energy spread	6 to 13 10^{-4}

Undulator/Optical klystron /20/

Overall length	1.3 m
Undulators 17 periods or 2 x 7 periods of 7.8 cm	
Dispersive section	70 < Nd < 100

Optical cavity /6/

Length	5.5 m
Mirrors radius of curvature	3 m
Mirrors transmission	3 10^{-5}
Cavity losses at 6500 Å	7 10^{-4} (first experiment)
	17 10^{-4} (after 40 runs)

FEL OSCILLATOR /1/

Typical duration after each injection	1 hour
Wavelength range	200 Å (first experiment)
around λ_L = 6500 Å	∿ 10 Å (after 40 runs)
Output average power at 180 MeV	200 μWatt at i = 50 mA
Output peak power (Q-switched)	∿ 2 Watt
Intracavity peak power (Q-switched)	50 KWatt
Intracavity peak power (Q-Switched)/cm^2	5 MWatt

12.4 - AVERAGE OUTPUT POWER OF THE SRFEL

We shall now examine the various characteristics of a FEL oscillator working on a storage ring. Since the only storage ring laser to have oscillated is the ACO machine at Orsay, and since we will refer to it through the rest of the text, we list its main characteristics in table III.

For further information, the reader may refer to /1/.

The average output power of the SRFEL has been first studied by RENVERI /27/ who solved the Fokker-Planck equation for the electron distribution function in the presence of the free electron laser. He found that the output power is limited to a small fraction of the synchrotron power emitted all around the ring :

$$P_{Laser} = \eta_c \chi \left(\frac{\Delta\omega}{\omega} \right) P_{synchr.} \qquad (12.24)$$

where $\left(\frac{\Delta\omega}{\omega} \right)$ is the homogeneous spontaneous emission linewidth (∿ 1/2N, where N is the nb of undulator pediods) and χ is an integral whose value is close to 1 for an undulator to 1.5 for a transverse gradient wiggler and to 1.2 for an optical klystron. η_c is the ratio transmission/losses of the cavity mirrors. Therefore, the maximum average power which can be extracted on a given storage ring (called "Renieri's limit") is :

$$P_L^{max} = \chi \left(\frac{\sigma_\gamma}{\gamma} \right)_{max} P_{synchr.} \qquad (12.25)$$

where $\left(\frac{\sigma_\gamma}{\gamma} \right)_{max}$ is the energy acceptance of the ring, whose order of magnitude is a few percent. A typical P_{synchr} on an XUV storage ring is 10 KWatt (Super ACO, 800 MeV). Of course, the gain must be high enough to reach this limiting power, and high gain requires long undulators which decrease the energy acceptance. The emitted power will be on the order of tens of watts in the Vis-UV spectral region and much less in the UV-XUV region where low energy acceptance undulators or optical klystrons will have to be used in order to maximize the gain (Remember that the gain drops with decreasing wavelength, for a given undulator, while the mirror losses become larger /22/).Together with a good energy acceptance, the power expressed in (12.25) can be reached only if the small-signal gain, g_o, is high enough compared to the saturated value of the gain, $g_s = \Gamma$ where Γ is the total optical cavity loss). There are several causes of saturation of the FEL :

- "Over bunching" which typically applies only for single pass FELs (See chapters 2, 5, 10 and 11).
- Saturation by increasing of the energy spread $\sigma_{\gamma/\gamma}$. At each pass through the undulator, the electron-light interaction increases the energy spread of the electron beam. This increase is counteracted

only by the synchrotron damping of the ring, which results in the Renieri limit for the emitted power.

- There is another cause of saturation which can prevent the Renieri limit to be reached. On storage rings the electron pulse RMS length is :

$$\sigma_z = \frac{\alpha c}{\omega_s}\left(\frac{\sigma_\gamma}{\gamma}\right) \qquad (12.23)$$

where ω_s is the synchrotron frequency, and α the momentum compaction factor /23/.

Then as the energy spread increases, σ increases and :

$g_o \sim \frac{1}{\sigma_z}$ since g_o is proportional to the electronic density. If one starts from a typical energy spread value of 5 10^{-4} and wants to reach 1 10^{-2} the gain/losses ratio has to be at least :

$$\frac{g_o}{\Gamma} > \frac{[\sigma_z]_{sat.}}{[\sigma_z]_{init.}} \simeq 20$$

Therefore the emitted power will decrease with the emitted wavelength (XUV region) since one will work with lower energy acceptance undulators or OK and with higher losses mirrors. In the case of the OK, assuming saturation by energy spread, the power has been explicitly calculated /24/ by using the energy spread evolution equation :

$$\frac{d}{dt}\,\Delta\left(\frac{\sigma_\gamma}{\gamma}\right)^2 = -\frac{2}{\tau_s}\,\Delta\left(\frac{\sigma_\gamma}{\gamma}\right)^2 + \frac{\langle(\delta\gamma)^2\rangle}{2T\gamma^2} \qquad (12.27)$$

= 0 at equilibrium

where $\Delta\left(\frac{\sigma_\gamma}{\gamma}\right)^2$ is the energy spread variation due to the FEL, τ_s the synchrotron damping time and T the ring round trip time. The laser induced energy spread $\langle(\delta\gamma)^2\rangle$ (second moment of the electron distribution) can be related to the net energy loss $\langle\delta\gamma\rangle$ by the Madey theorem /11/ (the SRFEL saturates in the small signal gain regime). Finally :

$$P_{OK} = \eta_c \frac{f}{\pi(N+N_d)}\,\frac{\mathrm{Log}(g_o/\Gamma)}{(g_o/\Gamma)}\,P_{synchr.} \qquad (12.28)$$

For the ACO SRFEL /1/ working at low energy $P_{synchr} \sim$ a few watts, $g_o/\Gamma \sim 2$, $N_d \sim 100$ and $\eta_c \sim 0.03$ so that the extracted power was very low, of the order of 5 10^{-5}. However the experimental value (of the order of 100 µwatts) was in very good agreement with the calculated value and exhibited a $\gamma^{4\pm0.7}$ dependence between 160 and 224 MeV, as expected from the Renieri's limit prediction since the synchrotron power varies as γ^4.

On super ACO the output power will vary between typically 100 mWatts (VUV laser running at 400 MeV with $N_d \sim 300$) and 50 Watts (visible laser, 800 MeV, undulator). Similar power levels are expected on the HIBESS storage ring.

12.5. PEAK POWER OF THE SRFEL - Q SWITCHING

The SRFEL has a pulsed structure, corresponding to the passage in the interaction region of one or several bunches stored in the ring. The typical duty cycle factor (bunch to bunch distance,T/bunch length) is 10^2. At laser saturation the light pulse is much narrow than the electron pulse ($l_L \sim \sqrt{l N \lambda_L}$, see below) by a factor of about 10^2. Therefore if the FEL was pseudo-cw, i.e., if it consisted in a series of pulses of same amplitude separated by T, its peak power would be approximately 10^4 times higher than the average value discussed above. In practice, it is easer to get a Q-switched than a pseudo-cw FEL. This leads to an increase of this factor by at least 1 order of magnitude (In the Q-switched mode of operation, the pulse length is larger than in the pseudo-cw operation. Therefore the power enhancement depends on the particular experimental conditions).

As the first SRFEL oscillator was obtained, on the storage ring ACO at Orsay /1/, it was observed that its temporal structure was, surprisingly,chaotic (fig. 3a). That is,the FEL pulse develops, with a risetime of the order of 0.5 msec, and then decreases. In this "natural" macrotemporal time structure each pulse train is separated from the following by a time interval varying randomly around an average value of typically 20 msec (depending on the experimental conditions). Meanwhile the emitted laser power did vary linearly with the stored current (fig. 4) indicating that this behavior was not due to threshold fluctuations (the difference between the optical gain and the cavity losses is of the order of 5 10^{-4}) and that FEL has reached saturation. This time structure is an intrinsic effect of the SRFEL. It has been explained by P. Elleaume /25/ by a very simple model.

By noticing that only small variations of energy spread, σ_γ/γ, are involved in the large variation of intensity versus time the equations (12.18) and (12.27) can be linearized giving the simple set of equations :

$$\begin{cases} \dfrac{dI}{dt} = \dfrac{(1-\Sigma)\, I}{\tau_o} \\[2ex] \dfrac{d\Sigma}{dt} = 2\,\dfrac{(1-\Sigma)}{\tau_s} \end{cases} \qquad (12.29)$$

where I is the laser power, $\Sigma = \sigma_\gamma^2 - \sigma_\gamma^2$ (laser off), both normalized to unity. τ_o is the laser rise time starting from the laser -off condition, $\tau_o = \frac{T}{g_o - \Gamma}$, i.e., τ_o can be understood as the rise time of the "first" laser pulse train once the gain has been set higher than the losses. τ_s is the synchrotron (damping) time. In general $\tau_o \ll \tau_s$ (For example on ACO, τ_o is typically $\sim$ 50 µsec and $\tau_s \sim$ 200 msec). This is likely to be the case for most of the SRFELs. τ_o will be shorter than on ACO (typically 1 µsec for $g_o - \Gamma = 0.1$), where the gain is very low but τ_s will also be shorter (typically 1-10 msec on most rings). Then the general solution of (12.29) is :

$$\Sigma = 1 + \Sigma_o\, e^{-t/\tau_s} \cos\left[\frac{2\pi(t-t_o)}{T_R}\right] \qquad (12.30)$$

where $T_R = 2\pi\sqrt{\frac{\tau_s\tau_o}{2}}$

The equations imply that the FEL tends to reach a stable equilibrium state after a series of damped oscillations of period T_R damped with the syncrhotron damping time τ_s . Numerical simulations show (fig. 5) that starting from the laser off condition the energy spread oscillates as in (12.30) while the laser intensity has a pulsed behavior before reaching a stable level. The shape of each pulse is approximated by :

$$\frac{I}{I_{max}} = ch^{-2}\left[\sqrt{\frac{I_{max}}{\tau_s\tau_o}}\,.\,t\right] \qquad (12.31)$$

$$I_{max} \simeq \frac{(1-\Sigma_i)\,\tau_s}{2\tau_o}$$

where Σ_i is the value of Σ at the "beginning" of the pulse. Moreover it can be shown that the equilibrium state is very unstable and resonnant with any perturbation of period close to T_R so that the laser has in practice a pulsed structure, as observed ($T_R \sim$ 15 msec on ACO). For example a noise of 3 % affecting the energy spread can account for the observed randomly pulsed behavior. On the whole this model fits very well the data obtained on ACO /1/. On fig. 6 are shown together the time evolution of a laser pulse and of the laser-induced energy spread, recorded by a bunch lengthening method /26, 27/. As predicted by the theory the energy spreads increases as the time-integral of the laser intensity. This points out the physical interpretation of the pulsed behavior : the laser pulse develops until the induced additional energy spread has driven the gain down to the level of the cavity losses. But then the laser pulse remains stored in the cavity and the energy spread continues to increase as the laser intensity slowly decreases. Therefore the gain is "killed" by the laser itself, and one needs some relaxation of the energy spread, with the "long" time constant τ_s, before the process starts again.

One interesting consequence of the laser instability is the possibility of Q-switching it. By modulating the optical gain with a period of the order of magnitude of T_R it is possible to obtain very regularly spaced and reproducible pulses (fig. 3b). Two methods have been used on ACO :

- Modulation of the storage ring revolution frequency in order to shift the overlap between the electron and light pulses. On ACO a 100 Hz difference with the nominal 13.6 MHz frequency was enough to turn off the laser. However this method has the disadvantage of inducing synchrotron oscillations on the energy spread.

- Periodic translation of the electron beam in the transverse direction inside the undulator. At Orsay, a displacement of .5 mm was sufficient to decrease the gain by a factor of 4. This method was the most efficient and reliable in the case of ACO.

Many other methods may be imagined.

The Q-switching of SRFEL has two great advantages over working with the "natural" structure :

(i) The laser is stabilized with a repetition rate of 10-100 Hz on ACO and 1-10 kHz on future experiments. It constitutes then a periodically pulsed source allowing the various accumulation or phase detection measurements methods. This is very important, both for the study of the laser itself (the fig. 5 was recorded under those conditions) and for the future users of SRFELs.

(ii) The laser peak power is enhanced by several orders of magnitude. If T_o is the Q-switching period a maximum is reached at $T_o \sim \tau_s$ and the power enhancement is about $\tau_s/4\tau_o$. This factor is $\sim 10^3$ for the Orsay experiment (and will be about the same on future experiments) although only 10^2 could be reached in practice (This is due to some particular features if the experiment /1/ which made it impossible to reach the low frequency, $T_o = \tau_s$, modulation regime). Remember that the higher the "small signal gain" g_o, the smaller the rise time τ_o and the bigger the peak power enhancement. However the estimates given above do not take into account saturation in the case of a high power SRFEL. When the dimensionless laser field /28/ :

$$a = \frac{4\pi \; Nc \; kL}{\gamma^2 \; mc^2} \qquad . \quad (12.30)$$

$\simeq 0.1$ on ACO (Q-switched regime), becomes of the order of unity overbunching will occur which will modify above results. Nevertheless we can conclude that the Q-switching will improve the usefulness of the SRFEL and their peak power by several orders of magnitude. Given the duty cycle of the ring, the narrowing of the laser micropulses and the expected Q-switching efficiency, the SRFEL peak power should lie at least in the MWatt range on future SRFELs.

To conclude this paragraph let us point out that "strange"

anomalous bunch lengthening behavior has been observed /1, 26/ on the ACO SRFEL. These effects have an important influence on its starts up behavior.Further analysis is needed to know if these phenomena will reappear in every storage ring FEL operated above the threshold current for the longitudinal field instability

12.6 - TRANSVERSE AND LONGITUDINAL MODE STRUCTURE

In the general case, gain is present over a range of transverse and longitudinal modes of the laser resonator cavity. In the presence of gain these modes are no longer the eigenmodes of the system, and the cross terms must be taken account of in a calculation of their evolution as a function of time. In the high gain case, both problems become complex.

As shown experimentally in /10/ and theoretically in /9/, the gain couples a single input transverse mode into many output modes. At low gain, the power emitted into the higher order modes is negligible ; as observed in all of the FEL oscillators to date, this produces a pure TEMoo output mode. In high gain systems, on the other band, the radiation from the FEL which mixes the modes dominates the initial power spectrum in the oscillator modes, and the output power will contain many modes. The mode content could perhaps be improved by using an adjustable iris placed inside the optical cavity /29/. In the very high gain regime, the cross terms which couple the growth of the modes can become so strong that the propagating wave no longer looks like any mode : the wave is actively guided /8/. In this case, a model analysis becomes inappropriate.

In the UV-vis spectral region the radiation can be extracted by either a partially transmitting mirrors or by a transparent plate oriented in the optical cavity near Brewster incidence. In the XUV region (λ_L < 1200 Å) it is very difficult to find transparent materials and the extraction must be performed by a mirror placed in the optical cavity slightly inside the optical mode. This will perturb the cavity modes and needs special theoretical attention.

The longitudinal structure (and therefore the spectral characteristics) of the laser are dominated by the problem of the "slippage" between the electron and light pulses. Due to the different velocities of the electron and light, the light pulse tends to shift in time with respect to the electron bunch. As a result the longitudinal eigenmodes of the laser are not the usual ones but the "supermodes" defined by Dattoli and Renieri /30/. The resulting laser pulse is Gaussian, of typical length ℓ_L, and its spectral with $\frac{\Delta\nu}{\nu}$ is transform limited :

$$\ell_L \simeq \ell\sqrt{\frac{s}{\ell}} = \sqrt{\ell N \lambda_L}$$

$$\frac{\Delta\nu}{\nu} \simeq \frac{1}{\pi}\frac{\lambda_L}{\ell_L} = \frac{1}{\pi}\sqrt{\frac{\lambda_L}{N\ell}} \qquad (12.33)$$

where ℓ is the initial bunch length and s the "slippage distance" ($= N\lambda_L$). N has to be replaced by $(N + N_d)$ in the case of the optical klystron. This predicts a relative spectral width of $5\ 10^{-5}$ for the ACO storage ring experiments, one order of magnitude narrower than the observed value ($\Delta\lambda_L \simeq 3$ Å for $\lambda_L \simeq 6\ 000$ Å).

Another approach has been given recently /31/ which leads to analytical solution for the supermodes. Their longitudinal distribution is then given by Hermite polynomials of order n. The lowest order mode, n = 1, corresponds to the Gaussian mode characterized in (12.33). Then one can follow the evolution of the laser time structure and take into account the incoherent emission stored inside the cavity. It is found that the line narrowing is limited to :

$$\Delta\lambda_L = \frac{\lambda_L^2}{2\pi s}\sqrt{\frac{I_o}{I_L}} \qquad (12.34)$$

where I_o is the stored spontaneous emission and I_L the laser intensity. For the ACO SRFEL, where the cavity Q is very high ($Q \sim 10^3$) and the gain very low (see table III) a high amount of spontaneous emission is stored and early saturation occurs so that /31/ :

$$\frac{I_L}{I_o} \simeq 40 \qquad (12.35$$

This leads to $\Delta\lambda \simeq 1.7$ Å. The remaining discrepancy with the observed value (3 Å) comes from energy oscillations which have been observed on the ring at low energy /27/. In future SRFEL with high gain and rather

high cavity losses the stored spontaneous emission is likely to be weak. However the emitted wavelength is very sensitive to small energy fluctuations ($\frac{\Delta\lambda}{\lambda} \sim 2\frac{\Delta\lambda}{\gamma}$) and it will be difficult to reach the limit defined in (12.33). A possible solution would be to insert a dispersive element, such as a Fabry-Perot etalon, inside the optical cavity. This appears to be extremely difficult since no such element exists at the present time in the VUV and XUV regions (except gratings which have very high losses).

12.7 - MIRROR DEGRADATION PROBLEM

Undulators placed on storage rings are today the most intense sources of XUV radiation /32, 33/. The FEL cavity mirrors placed in an optical cavity in front of the undulator is subject to an extremely intense bombardment of photons (fig. 7) of various wavelengths, particularly for high K. This was a severe problem in the Orsay experiment, even at low energy. In this case the problem was solved /1, 6/ by
(i) working at lower K than the initially designed value (fig. 7),
(ii) using the best available mirrors (made with SiO_2/TiO_2 multilayers),
(iii) working at the designed wavelength of these mirrors. The observed degradation occured mainly at the surface so that the reflectivity at the design wavelength of the multilayer stack was little changed, as can be seen from figure 8. However this effect restricted greatly the tunability of the laser (see Table III). In addition to the single photon degradation effects, there is a difficult heating problem.

The total power emitted by an undulator is :

$$P(\text{watt}) = 7.3\ E^2(\text{GeV}).I(A).N.K^2/\lambda_o\ (\text{cm}) \qquad (12.36)$$

For the undulator listed in Table I this gives, for a stored current of 0.1 Amp., a total power of 1 kWatt. Approximately half of this would hit a 25 mm wide mirror placed 50 m apart from the center of the undulator. Mirror degradation and heating by the spontaneous power (not to mention the stored power) will have to be considered very seriously in the future. Unfortunately, very little degradation data is available today in the UV to XUV spectral regions /22/.

12.8 - CONCLUSION

Today half-a-dozen of SRFEL projects are currently underway :

- On ACO at Orsay, the studies are continuing /1/.
- At Frascati, where the first measurements of the gain on the harmonics were performed, a vis FEL is under construction /3/.
- At Brookhaven a UV-vis FEL is being planned /4/.
- At Novossibirsk /2/, where the first data on the optical klystron have been obtained, optical gains on the order of several percent have been demonstrated. The mirror degradation problem has prevented laser oscillation so far.
- At Berlin an isochronous storage ring laser at $\lambda = 500 - 200\ \mu$ is under construction /16, 34/.
- A project on super-ACO, as explained above, will start in 1986-87.
- At Stanford, a FEL dedicated storage ring is under construction /14/. This project will be able to reach the XUV region ($\lambda < 1000$ Å)
- At Tsukuba a synchrotron radiation FEL ring very similar to the Stanford ring is under construction /35/.
- At Berkeley a storage ring using a "by-pass" working in the high gain regime has been proposed /17/.

We can conclude from our present study that much work has been done both theoretically and experimentally on the SRFEL. Its feasibility has been proven by its successful operation on the storage ring ACO at Orsay.

But theoretically and experimentally, a wide range of problems requires more effort. It has become very clear that the ultimate performance of the storage ring FEL depends strongly on the quality of the electron beam. In addition to the laser work, significant effort should be applied to the general question of obtaining high current low emittance beams in storage rings. On the laser side, the outstanding issues include the high gain regime and its mode characteristics, both transverse and longitudinal ; very short wavelength operation and the present technological limits ; the overbunched regime in the presence of Q-switching ; and the performance of the laser above the anomalous

bunch lengthening threshold. The experimental issues in constructing long undulators /36/ with field tolerances must be addressed, the degradation characteristics and heat transport in the candidate mirror materials and substrates must be measured, and the high current and low emittance required for UV operation must be obtained.

The ultimate limits on the FEL performance depend on what is possible in several crucial technologies. As we have discussed in this review, these technologies are : 1) high brightness electron beam, 2) long undulator technology, and 3) optics, including degradation, heating, and XUV technology. Each of these technological areas will pay dividends of better FEL performance as progress is made.

Based on the knowledge of the FEL interaction produced in these centers over the past few years, we can confidently predict operation of the FEL at wavelengths as short as 1000 Å. As progress is made on the outstanding technical issues, it may become possible to produce coherent radiation at wavelengths below 100 Å. However this will take years and the minimum wavelength of FEL operating on to-day existing storage rings (mostly in synchrotron radiation facilities) will be approximately 1 200 Å (limit of the Al coatings). For that reason, several synchrotron radiations centers (Brookhaven, Orsay ...) have become interested in the technique of harmonic generation by using an optical klystron /37/. This technique of XUV production, recently demonstrated at Orsay /38/, could allow to-day existing rings to provide coherent light down to about 300 Å, while the research will continue on the potentially more powerful FEL oscillators.

FIGURE CAPTIONS

Fig. 12.1 - Small signal gain calculated as a function of wavelength from the small signal gain formula for several different undulator wavelengths. These values of gain must be increased to take account of the effects of high gain : exponential growth, reduced sensitivity to beam quality, and active guiding.

Fig. 12.2 - Comparison /12/ of the measured gain spectrum with the derivative of the spontaneous radiation spectrum.

Fig. 12.3 - Time recording of the laser intensity for :

- a- "Natural" operation
- b - Low frequency Q-switched operation. The lower trace is the trigger signal. The total time interval is 200 msec. The sensitivity on "b" is x 4 less than on "a".

Fig. 12.4 - Average laser power and ring current recorded together versus time after injection of the ring. The ratio of the two quantities is a constant on most of the laser operation range.

Fig. 12.5 - Dimensionless energy spread evolution obtained with (see text and ref. /23/) $\tau_o/\tau_s = 0.25$ and $I = 10^{-5}$ and $\Sigma = 0$ at $t = 0$.

Fig. 12.6 - Time recording of the laser intensity (upper trace) together with the bunch length evolution (lower trace). A negative signal corresponds to a lengthening of the bunch. The total time interval is 100 msec for the left picture and 5 msec for the right one.

Fig. 12.7 - Number of photons hitting the front FEL mirror in the Orsay experiment /1/ with respect to the harmonic number of the spontaneous emission line. In this graph the fundamental emission line is held constant (at $\lambda = 650$ nm) which implies to lower the parameter K as the energy is decreased, as indicated in the table. It appears that the harmonic content is minimized, at K = 0.7 and E = 155 MeV (Minimum working energy of the ACO storage ring).

Fig. 12.8 - Mirror degradation after exposition to the VUV undulator radiation. T_r is the transmission (unaffected by the UV exposure). Points (a) and (a') correspond to measurement of the average mirror losses $\Gamma = 1 - \bar{R}$ with an He-Ne laser respectively before and after insertion in the vacuum. Curve (b) corresponds to measurements done after an exposition of a few minutes at 150 MeV and curve (c) to an exposition of 1 Amp-hour at 166 MeV. Measurements methods are described in ref. /16/.

REFERENCES

/1/ M. Billardon, P. Elleaume, J.M. Ortega, C. Bazin, M. Bergher, M. Velghe, Y. Petroff; D.A.G. Deacon, K.E. Robinson and J.M.J. Madey, Phys. Rev. Lett. 51, 1652 (1983).

P. Elleaume, J.M. Ortega, M. Billardon, C. Bazin, M. Bergher, M. Velghe, Y. Petroff, D.A.G. Deacon, K.E. Robinson, J.M.J. Madey, J. Phys., 45, 989 (1984).

M. Billardon, P. Elleaume, J.M. Ortega, C. Bazin, M. Bergher, Y. Petroff, M. Velghe. to be published in Nucl. Instr. & Meth. (1985), special issue on the proceedings of the Castelgondolfo FEL Conference?

/2/ N. Vinckurov To be published in Nucl. Instr. & Meth. (1985) special issue on the proceedings of the Castelgondofo FEL conference.

/3/ M. Biagini, R. Boni, S. De Simone, S. Guiducci, M. Preger, M. Serio, S. Tazzari, F. Tazzari, S. Trillo; M. Vescovi, M. Ambrosio, G.C. Barbavino, M. Castellano, N. Cavello, F. Cevenini, M.R. Masullo, P. Putteri, R. Rinzivillo, S. Solimeno, in "Free Electron Generators of Coherent Radiation" (Brau, Jacobs, Scully, eds.) Proc. SPIE 453, 295 (1984).

/4/ S. Krinsky, A. Luccio, C. Pellegrini, A. Van Steenbergen, L.H. Yu, in Proceedings of the BENDOR FEL Conference (Billardon, Deacon, eds.). J. de Phys., C1-113 (1983).

/5/ Proceedings of the Castelgondolfo workshop on the applications of free electron lasers (Deacon, De Angelis, Eds.), to be published in Applied Optics (1985).

/6/ P. Elleaume, M. Velghe, M. Billardon, J.M. Ortega, J. of Optics 15, 262 (1984).

P. Elleaume, M. Velghe, M. Billardon, J.M. Ortega, to be published in Applied Optics (1985).

also in ref. /5/.

/7/ D. Attwood et al., "Free Electron Generators of Extreme Ultraviolet Coherent Radiation"(Madey, Pellegrini, eds.) AIP Conference Proceedings 118-4, 294 (1984).

/8/ E.T. Scharleman, A.M. Sessler, J.S. Wurtele, UCRL-91476, Preprint Lawrence Livermore National Laboratory, to be published in Phys. Rev. Lett. (1985).

/9/ P. Elleaume, D.A.G. Deacon, Appl. Phys. B, 33, 9 (1984).

/10/ W.B. Colson and P. Elleaume, Appl. Phys. B 29, 101 (1982).

/11/ J.M.J. Madey, Nuovo Cimento, 50 B, 64 (1979).

/12/ D.A.G. Deacon, K.E. Robinson, J.M.J. Madey, C. Bazin, M. Billardon, P. Elleaume, Y. Farge, J.M. Ortega, Y. Petroff, M.F. Velghe, Opt. Commun. 40, 373 (1982).

/13/ N.A. Vinokerov and A.N. Skrinski, Preprint INP 77, 59 Novossibirsk (1977).

See also N.A. Vinokurov, Proc. Xth Intl. Cong. on High Energy Charge Particle Accelerators, Serpukhov, vol. 2, 454 (1977).

/14/ J.M.J. Madey, in "Proceedings of the BENDOR FEL Conference", (Billardon, Deacon, eds.) Journ. de Phys. 44, C1-169 (1983).

/15/ D.A.G. Deacon, Physics Reports 76, 351 (1981).

/16/ A. Gaupp, in "Proceedings of the BENDOR FEL Conference" (Billardon, Deacon, eds.) Journ. de Phys. 44, C1-147 (1983).

/17/ J. P. Murphy and C. Pellegrini, BNL-34886 Preprint, Brookhaven National Laboratories, to be published in Optics Communications (1984).

/18/ P. Elleaume, J. Physique Colloq. 44, C1-333 (1983), and Physics of Quantum Electronics, vol. 8, ch. 5 (Addison-Wesley, New-York) (1982).

/19/ M.P. Level, "Service Anneaux de Collision". Int. Rep. NI-04-84 and private communication.

/20/ J.M. Ortega, C. Bazin, D. Deacon, C. Depautex, Nucl. Instr & Meth. 206, 281 (1983).

J.M. Ortega, C. Bazin, D. Deacon, J. Appl. Phys. 54, 4776 (1983).

/21/ A. Renieri, Nuovo Cimento, 53 B, 160 (1979).

/22/ Ref. 7 and D.T. Attwood, chap. 16, This volume.

/23/ M. Sands, SLAC report n° 121 (1970), Stanford, California.
A. Van Steenbergen, chap. 14, This volume.

/24/ P. Elleaume, "Storage ring FEL Theory", FEL Conference Castelgandolfo (1984). To be published in N.I.M. (1985) and Thesis - Université Paris-Sud, 1984 (Rapport CEA-R-5279 Saclay).
See also ref. /1/.

/25/ P. Elleaume, J. de Physique, 45, 997 (1984).

/26/ K.E. Robinson, D. Deacon, M. Velghe, J. Madey, IEEE J. Quant. Electr. QE-19, 365 (1983).
K.E. Robinson, Thesis, Stanford (1984).

/27/ J.M. Ortega, P. Elleaume, M. Billardon, D. Deacon, B. Girard, Y. Lapierre. FEL Conference, Castelgandolfo (1984) - To be published in N.I.M. (1985).

/28/ W.B. Colson. Phys. of Quantum Electronics, Vol. 8, 457 (1982) and Chapter 5. This volume.

/29/ M. Velghe, D. Deacon, J.M. Ortega, Applied Optics, 23, 3851 (1984).

/30/ G. Dattoli and A. Renieri, Nuovo Cimento, 59 B, 1 (1980).

/31/ P. Elleaume, FEL Conference. Castelgandolfo (1984), To be published in N.I.M. (1985).

/32/ S. Krinsky, N.I.M. 172, 73 (1980).
J.M. Ortega, M. Billardon, J. Gezequel, P. Thiry, Y. Petroff, Le Journal de Physique, 45, 1883 (1984).

/33/ P. Elleaume, This volume, chapter 5.

/34/ A. Gaupp in ref. /5/

/35/

/36/ K. Halbach This volume, Chapter 5.

/37/ F. De Martini, This volume, chapter 7.

/38/ B. Girard, Y. Lapierre, J.M. Ortega, C. Bazin, M. Billardon, P. Elleaume, M. Bergher, M. Velghe, Y. Petroff, Phys. Rev. Lett. 53, 2405 (1984).
J.M. Ortega, Y. Lapierre, B. Girard, M. Billardon, P. Elleaume, C. Bazin, M. Bergher, M. Velghe, Y. Petroff, IEEE, J. of Quantum Electronics, to be published in Special Issue on FEL (July 1985).

5260-1

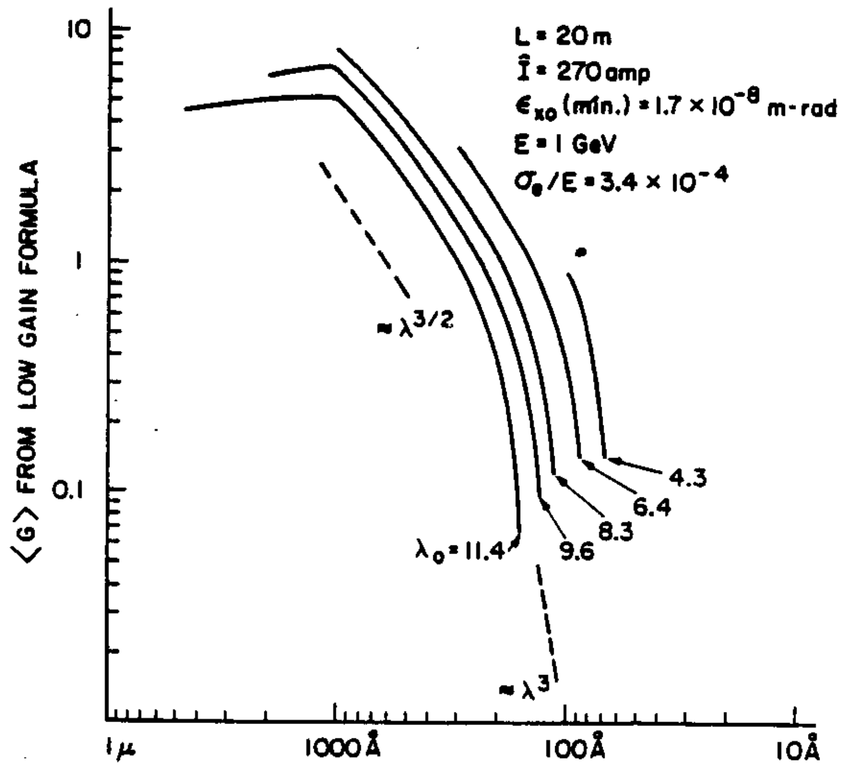

1

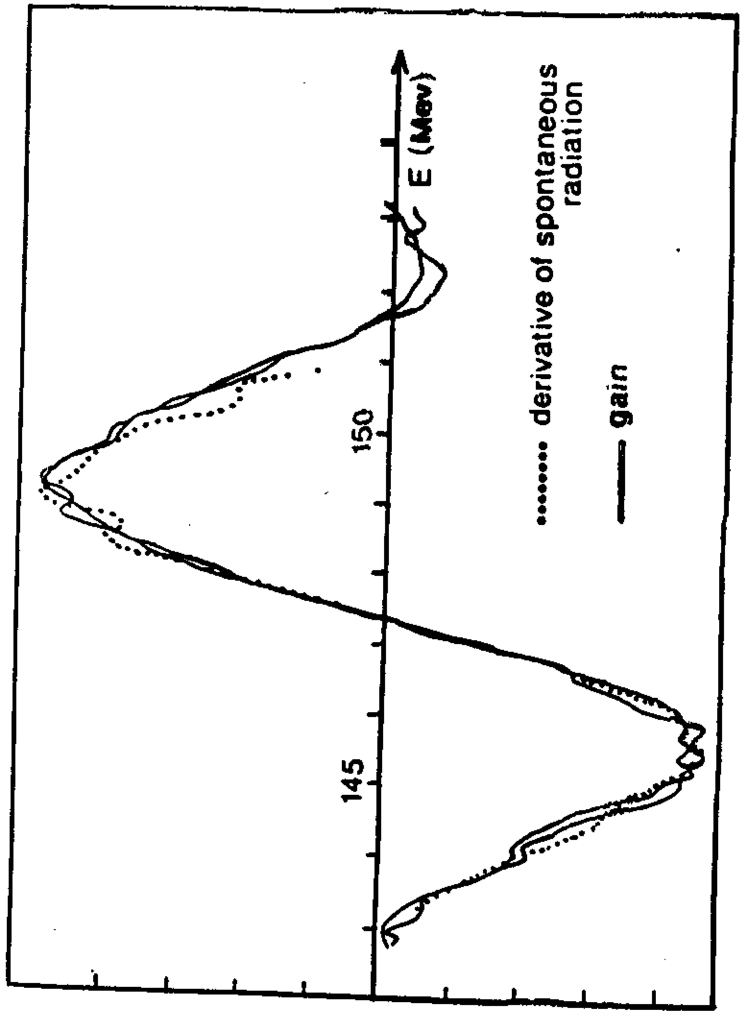

Figure 2

- a -

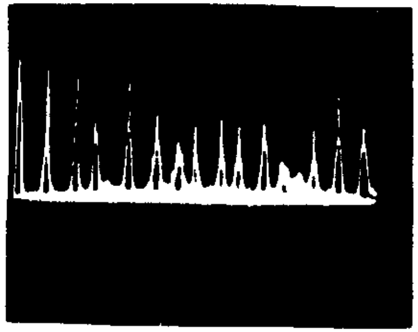

- b -

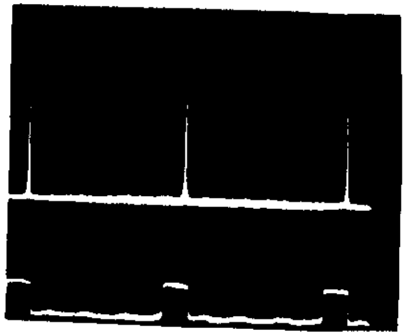

Fig 12-3

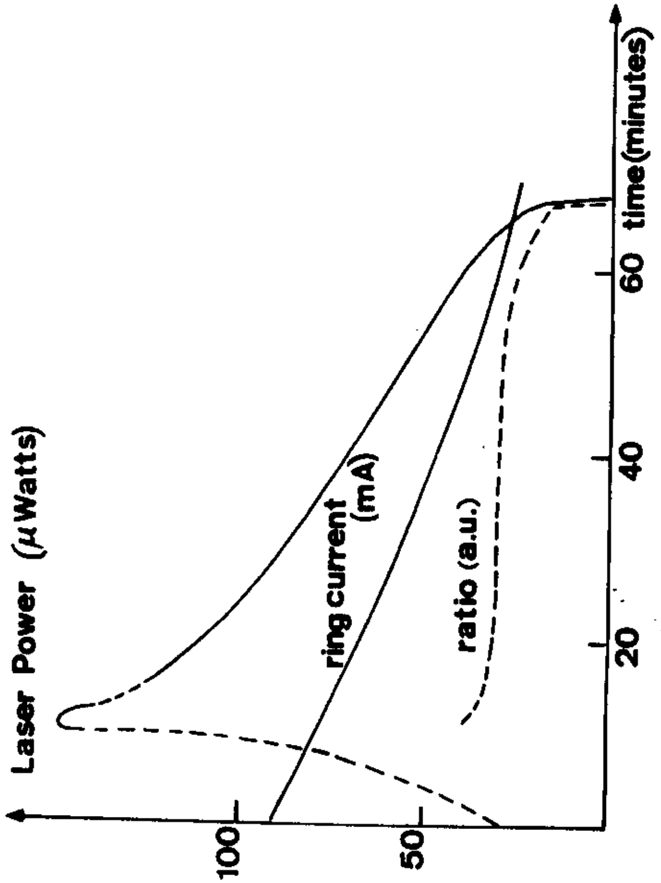

Fig. 12-4

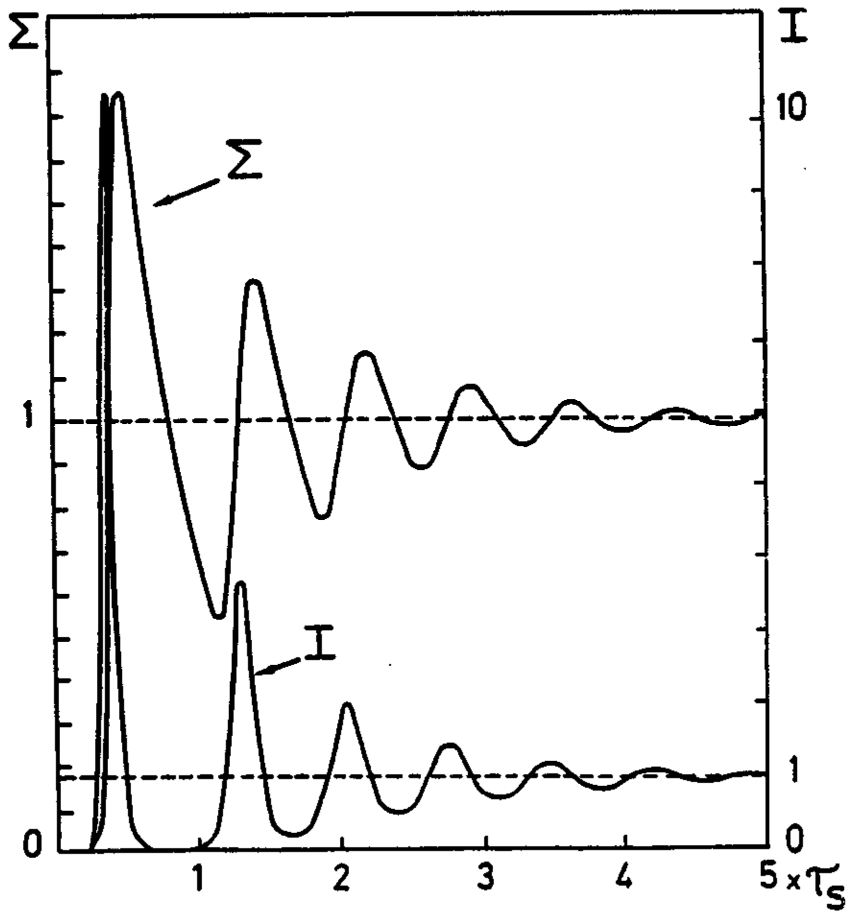

Fig 12-5

(right)

(left)

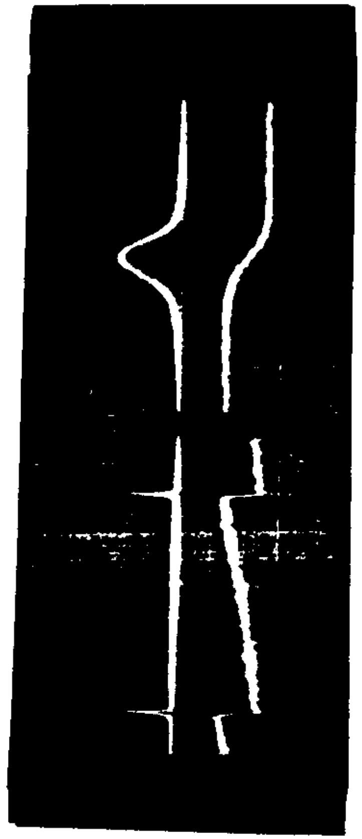

Fig 12-6

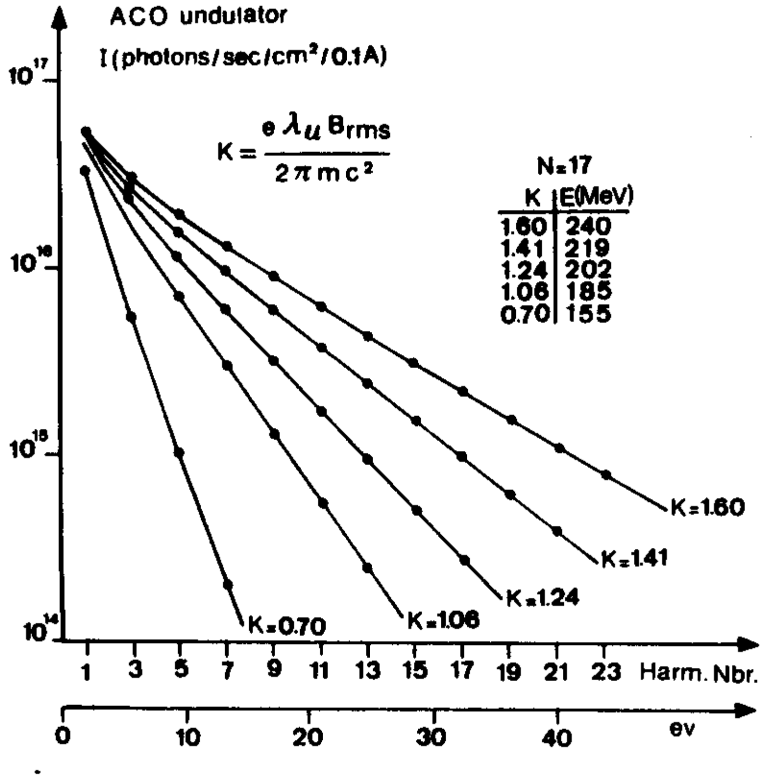

Fig. 12-7

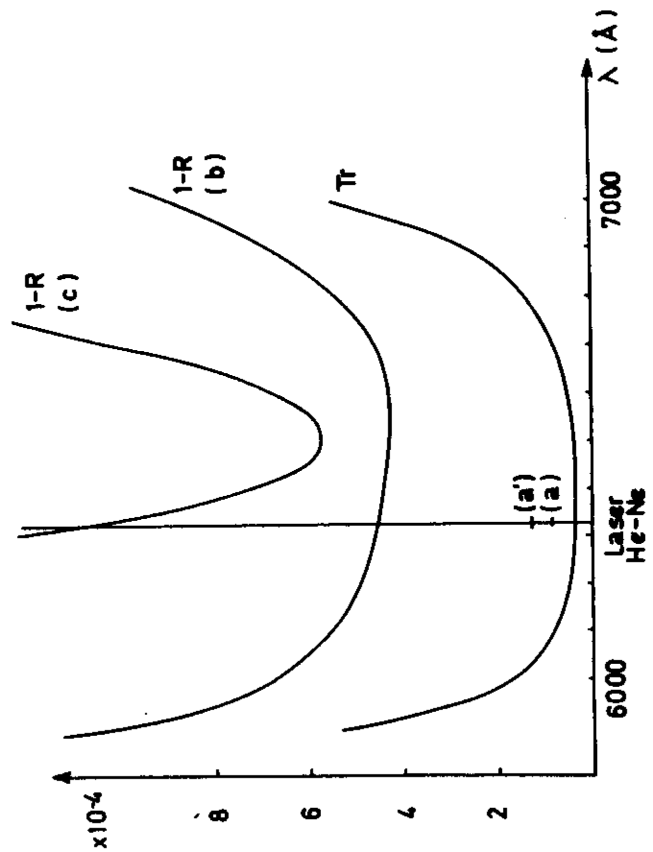

Fig. 12-8